

Charged-particle production in Pb+Pb and Xe+Xe collisions measured with the ATLAS detector

Petr Balek^{*†}

Weizmann Institute of Science, Rehovot, Israel

E-mail: petr.balek@cern.ch

Measurements of charged-particle production in heavy-ion collisions and their comparison to pp data provide insight into the properties of the quark-gluon plasma. In 2015, the ATLAS detector at the LHC recorded 0.49 nb^{-1} of Pb+Pb collisions and 25 pb^{-1} of pp collisions at a center-of-mass energy of $\sqrt{s_{NN}} = \sqrt{s} = 5.02 \text{ TeV}$. In addition, around $3 \mu\text{b}^{-1}$ of Xe+Xe collisions at $\sqrt{s_{NN}} = 5.44 \text{ TeV}$ were recorded in 2017. These samples provide an opportunity to study the dependence of the parton energy loss over the system size. The large acceptance of the ATLAS detector allows measurements of charged-particle spectra in a wide range of both pseudorapidity and transverse momentum, and differential in collision centrality. Charged-particle spectra measured in Pb+Pb and Xe+Xe collisions are compared to the analogous spectra measured in pp collisions, and the resulting nuclear modification factors are scrutinized. In particular, the nuclear modification factors are found to scale approximately with the number of participating nucleons, which may be a key to predicting the behavior of even smaller collision systems.

*International Conference on Hard and Electromagnetic Probes of High-Energy Nuclear Collisions
30 September - 5 October 2018
Aix-Les-Bains, Savoie, France*

^{*}Speaker.

[†]on behalf of the ATLAS collaboration



1. Introduction

Yields of charged hadrons are suppressed in the Pb+Pb collisions relative to the pp collisions [1, 2, 3, 4, 5, 6]. The Xe+Xe collisions at similar center-of-mass energy offer an opportunity to study properties of the quark-gluon plasma in the system with different geometry [7, 8]. The suppression of charged-hadron production is quantified using the nuclear modification factor R_{AA} :

$$R_{AA} = \frac{1}{\langle T_{AA} \rangle} \frac{1/N_{\text{evt}} dN_{\text{ch}}/dp_T}{d\sigma_{pp}/dp_T},$$

where $1/N_{\text{evt}} dN_{\text{ch}}/dp_T$ is the yield of charged hadrons measured per Xe+Xe or Pb+Pb event differentially in transverse momentum p_T ; $d\sigma_{pp}/dp_T$ is the differential pp cross-section; and $\langle T_{AA} \rangle$ is the nuclear thickness function accounting for an increased parton flux in the Xe+Xe or Pb+Pb collisions with respect to the pp collisions.

2. Analysis

The measurement of the charged hadrons production uses data recorded by the ATLAS detector [9]. The tracking information is provided by the inner detector which covers $|\eta| < 2.5$ and which is immersed in a 2 T axial magnetic field. The calorimeter system consists of an electromagnetic calorimeter covering $|\eta| < 3.2$, hadronic calorimeters covering also $|\eta| < 3.2$ and forward calorimeters covering $3.1 < |\eta| < 4.9$. The muon spectrometer covers $|\eta| < 2.7$.

The analysis of the Xe+Xe collisions [10] uses total integrated luminosity of $3 \mu\text{b}^{-1}$ recorded in collisions with the center-of-mass energy of $\sqrt{s_{NN}} = 5.44$ TeV. The Xe+Xe events are required to have at least one track reconstructed in the inner detector or the total transverse energy deposited in the calorimeters had to exceed 4 GeV. The pp cross-section is obtained from extrapolation of the $\sqrt{s} = 5.02$ TeV data [2] to the same center-of-mass energy.

The total transverse energy in the forward calorimeters (FCal E_T) is used to characterize the centrality of a collision. By convention, the centrality is measured in percentiles of the total inelastic cross-section. Collisions with a large overlap between nuclei are called ‘‘central’’ and are assigned small centrality values, while collisions with small overlap are called ‘‘peripheral’’ and have centrality closer to 100%. The geometric parameters of collisions for each centrality interval are estimated using the Glauber Monte Carlo model [11, 12]; those are the number of nucleons participating in the collision, N_{part} , the number of binary nucleon–nucleon collisions, N_{coll} , the nuclear thickness function, T_{AA} , as well as their uncertainties.

A particle originating in the initial collision typically crosses four layers of the pixel detector, four double-sided modules of the semiconductor tracker and around 36 straw tubes of the transition radiation tracker. A track is required to be of good quality and also to emerge from the collision vertex; details are provided in Ref. [10]. A track with $p_T > 40$ GeV is further required to be matched to a jet within $\Delta R = \sqrt{\Delta^2\eta + \Delta^2\phi} < 0.4$. The jets are reconstructed using anti- k_t algorithm [13] with the radius parameter $R = 0.4$.

The detector response effects are studied using Monte Carlo simulations. Hard-scattering pp collisions generated by PYTHIA 8 [14] are overlaid onto Xe+Xe collisions produced by HIJING [15]. The resulting events are reconstructed in the same way as data.

There are several corrections applied to the measured spectra. First, secondary and fake tracks are subtracted. The former ones are tracks matched to secondary particles, and the later ones are the tracks that are coming from the spurious combination of hits not associated with a single particle. Leptons from the decays of electroweak bosons are subtracted as well because they do not follow the same suppression pattern as hadrons [16]. The spectra are then corrected for the p_T resolution and for the track reconstruction efficiency by the bin-by-bin unfolding.

The pp cross-section measured at $\sqrt{s} = 5.02$ TeV is extrapolated to $\sqrt{s} = 5.44$ TeV by the ratio of the charged hadron spectra generated by PYTHIA 8.

There are several sources of the systematic uncertainties affecting the results. The analysis parameters are varied independently and the resulting outcomes are compared to that of the default setup. The correlated components are varied consistently in numerator and denominator in order to estimate the uncertainty on R_{AA} . The highest systematic uncertainties come from limited statistics of the simulation samples, a limited description of the inactive material of the detector, and variations of the track selection requirements. Significant uncertainties are also those of the geometric parameter $\langle T_{AA} \rangle$ and the pp cross-sections extrapolation.

3. Results

The nuclear modification factors, R_{AA} , for Xe+Xe and Pb+Pb collisions in the same centrality intervals are shown in the left panel of Figure 1; the results for Pb+Pb collisions were presented in Ref. [2]. Both curves have a similar shape: they reach a maximum at $p_T \approx 2$ GeV, then a minimum at around 7 GeV and then increase up to around 60 GeV. The shape is more pronounced in the central collisions. The behavior of R_{AA} in Xe+Xe collisions above 60 GeV is difficult to ascertain due to the low statistics. In Pb+Pb collisions, the slope of R_{AA} for $p_T \gtrsim 60$ GeV certainly diminishes. The stronger suppression in Pb+Pb than in Xe+Xe collisions for the same centrality intervals is expected because the size of a Pb+Pb collision system is larger than that of a Xe+Xe collision. The right panel of Figure 1 shows R_{AA} in Xe+Xe and Pb+Pb collisions in different centrality intervals but having similar FCal E_T . The system formed in collisions with similar FCal E_T have approximately the same size for Xe+Xe and Pb+Pb. The observed suppressions are consistent between the two systems within the systematics uncertainties, suggesting scaling with the system size.

Figure 2 shows comparison of nuclear modification factors for Xe+Xe and Pb+Pb collisions for centrality intervals of similar $\langle N_{part} \rangle$ (left) and $\langle N_{coll} \rangle$ (right). The production rate of low- p_T (high- p_T) particles is expected to be approximately proportional to N_{part} (N_{coll}). The size of the system is expected to scale better with the N_{part} than with the N_{coll} , but it is noticeable that the agreement between the two systems in both cases is still worse than in case of FCal E_T . At p_T around 7 GeV, the Xe+Xe results on the left panel of Figure 2 show slightly stronger suppression for the central events, but slightly milder suppression for peripheral events. This feature is demonstrated in Figure 3 where it is clearly visible. In the p_T range 26–30 GeV, the suppressions are comparable within uncertainties and R_{AA} measured in both Xe+Xe and Pb+Pb collisions follow the same dependency, which suggests the suppression scales with the system size.

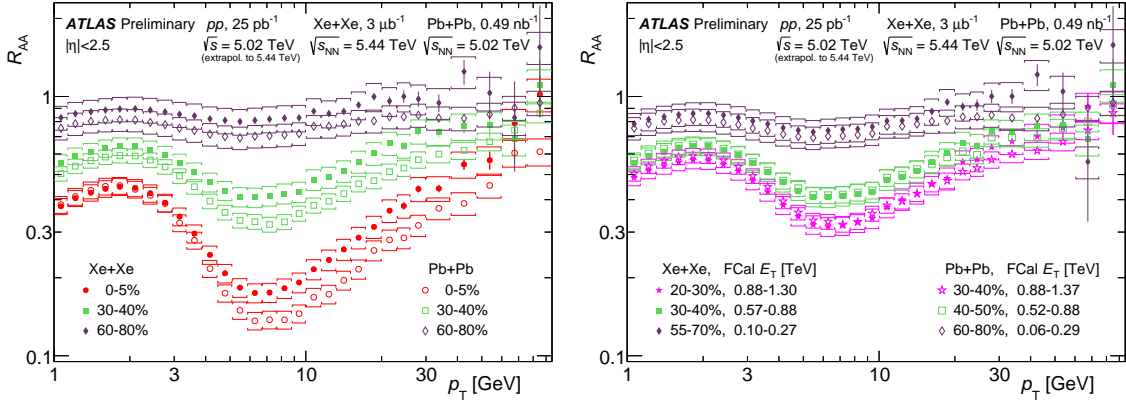


Figure 1: Nuclear modification factors R_{AA} as a function of p_T measured in Xe+Xe collisions (closed markers) and in Pb+Pb collisions (open markers) [10]. The intervals of the same marker styles have the same centrality (left) or comparable deposited energy in the forward calorimeter (right). The statistical uncertainties are shown as the bars; systematic uncertainties are shown by the brackets.

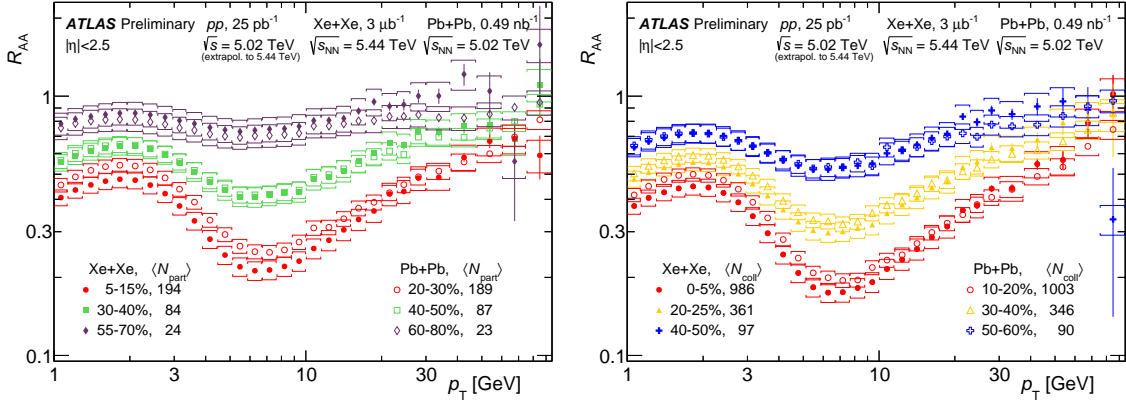


Figure 2: Nuclear modification factors R_{AA} as a function of p_T measured in Xe+Xe collisions (closed markers) and in Pb+Pb collisions (open markers) [10]. The centrality intervals of the same marker styles have comparable $\langle N_{part} \rangle$ (left) or $\langle N_{coll} \rangle$ (right). The statistical uncertainties are shown as the bars; systematic uncertainties are shown by the brackets.

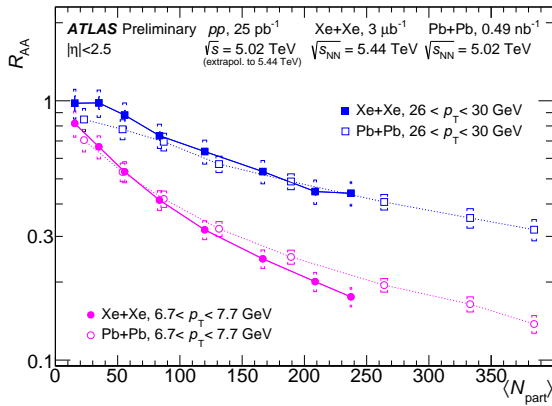


Figure 3: Nuclear modification factors R_{AA} as a function of N_{part} for two selected p_T ranges measured in Xe+Xe collisions (closed markers) and in Pb+Pb collisions (open markers) [10]. The statistical uncertainties are shown as the bars, and systematic uncertainties are shown by the brackets. The width of the brackets represents the systematic uncertainty of N_{part} . The lines are only to help guide the eye.

4. Summary

Measurement of charged-hadron spectra and the nuclear modification factor in Xe+Xe collisions has been presented. The R_{AA} is compared between the Xe+Xe collisions at $\sqrt{s_{NN}} = 5.44$ TeV and Pb+Pb collisions at $\sqrt{s_{NN}} = 5.02$ TeV measured by the ATLAS detector at the LHC.

The data suggest that R_{AA} scales with the system size. Other aspects of the collisions, such as center-of-mass energy or initial energy density, may not play a significant role in the comparison presented in this proceedings. However, they may become important when comparing collisions at the LHC energies to those at e.g. RHIC energies.

Acknowledgement

This research is supported by the Israel Science Foundation (grant 1065/15) and by the MINERVA Stiftung with the funds from the BMBF of the Federal Republic of Germany.

References

- [1] ATLAS Collaboration. *JHEP* **09** (2015) 050 [1504.04337].
- [2] ATLAS Collaboration. *ATLAS-CONF-2017-012* [<https://cds.cern.ch/record/2244824>].
- [3] CMS Collaboration. *Eur. Phys. J.* **C72** (2012) 1945 [1202.2554].
- [4] CMS Collaboration. *JHEP* **04** (2017) 039 [1611.01664].
- [5] ALICE Collaboration. *Phys. Lett.* **B720** (2013) 52 [1208.2711].
- [6] ALICE Collaboration. *JHEP* **11** (2018) 013 [1802.09145].
- [7] G.-Y. Qin and X.-N. Wang. *Int. J. Mod. Phys. E* **24** (2015) 1530014 [1511.00790].
- [8] Y. Mehtar-Tani, J. G. Milhano and K. Tywoniuk. *Int. J. Mod. Phys. A* **28** (2013) 1340013 [1302.2579].
- [9] ATLAS Collaboration. *JINST* **3** (2008) S08003.
- [10] ATLAS Collaboration. *ATLAS-CONF-2018-007* [<https://cds.cern.ch/record/2318588>].
- [11] M. L. Miller et al. *Ann. Rev. Nucl. Part. Sci.* **57** (2007) 205 [nucl-ex/0701025].
- [12] C. Loizides, J. Nagle and P. Steinberg. *SoftwareX* **1–2** (2015) 13 [1408.2549].
- [13] M. Cacciari, G. P. Salam and G. Soyez. *JHEP* **04** (2008) 063 [0802.1189].
- [14] T. Sjöstrand et al. *Comput. Phys. Commun.* **191** (2015) 159 [1410.3012].
- [15] X.-N. Wang and M. Gyulassy. *Phys. Rev. D* **44** (1991) 3501.
- [16] ATLAS Collaboration. *ATLAS-CONF-2017-010* [<https://cds.cern.ch/record/2244821>].